JBC RESEARCH ARTICLE

Modulation of galectin-9 mediated responses in monocytes and T-cells by pregnancy-specific glycoprotein 1

Received for publication, May 20, 2024, and in revised form, July 16, 2024 Published, Papers in Press, August 8, 2024,
https://doi.org/10.1016/j.jbc.2024.107638

Mirian Mendoza[1,‡], Angela Ballesteros[2,‡], Elizabeth Rendon-Correa[1], Rohan Tonk[2], James Warren[1], Andrew L. Snow[3], Sean R. Stowell[4], Sandra M. Blois[5,6], and Gabriela Dveksler[1,*]

From the [1]Department of Pathology, Uniformed Services University of the Health Sciences, Bethesda, Maryland, USA; [2]Section on Sensory Physiology and Biophysics, National Institute on Deafness and other Communication Disorders, National Institutes of Health, Bethesda, Maryland, USA; [3]Department of Pharmacology and Molecular Therapeutics, Uniformed Services University of the Health Sciences, Bethesda, Maryland, USA; [4]Department of Pathology, Brigham and Women's Hospital, Boston Massachusetts, USA; [5]Department of Obstetrics and Fetal Medicine, University Medical Center Hamburg-Eppendorf, Hamburg, Germany; [6]Glyco-HAM, a cooperation of Universität Hamburg, Technology Platform Mass Spectrometry and University Medical Center Hamburg-Eppendorf, Hamburg, Germany

Reviewed by members of the JBC Editorial Board. Edited by Robert Haltiwanger

Successful pregnancy relies on a coordinated interplay between endocrine, immune, and metabolic processes to sustain fetal growth and development. The orchestration of these processes involves multiple signaling pathways driving cell proliferation, differentiation, angiogenesis, and immune regulation necessary for a healthy pregnancy. Among the molecules supporting placental development and maternal tolerance, the families of pregnancy-specific glycoproteins and galectins are of great interest in reproductive biology. We previously found that PSG1 can bind to galectin-1 (GAL-1). Herein, we characterized the interaction between PSG1 and other members of the galectin family expressed during pregnancy, including galectin-3, -7, -9, and -13 (GAL-3, GAL-7, GAL-9, and GAL-13). We observed that PSG1 binds to GAL-1, -3, and -9, with the highest apparent affinity seen for GAL-9, and that the interaction of PSG1 with GAL-9 is carbohydrate-dependent. We further investigated the ability of PSG1 to regulate GAL-9 responses in human monocytes, a murine macrophage cell line, and T-cells, and determined whether PSG1 binds to both carbohydrate recognition domains of GAL-9. Additionally, we compared the apparent affinity of GAL-9 binding to PSG1 with other known GAL-9 ligands in these cells, Tim-3 and CD44. Lastly, we explored functional conservation between murine and human PSGs by determining that Psg23, a highly expressed member of the murine Psg family, can bind some murine galectins despite differences in amino acid composition and domain structure.

A healthy pregnancy requires the coordination and regulation of a series of biological processes occurring at both sides of the maternal-fetal interface, including vascular development and remodeling, immune regulation, placental invasion, and placental growth (1). Multiple mediators secreted from both the mother and the fetus orchestrate these processes, including members of the galectin family. Galectins are β-galactoside binding proteins that modulate cell adhesion, migration, immune function, placentation, and angiogenesis either intracellularly or when secreted into the extracellular space (1, 2). Some galectins are expressed widely at the maternal-fetal interface, while the expression of others is highly specific to certain trophoblast populations or maternal cell types. Galectins in this category include galectin 1 (GAL-1), galectin 3 (GAL-3), galectin 9 (GAL-9), galectin 7 (GAL-7), and the placenta-specific galectin 13 (GAL-13), also known as placental protein 13 (PP13) (3–18). Some of the ligands for these galectins have been characterized and are known to play important roles in several biological processes required for successful pregnancy as previously summarized (2, 19).

The maternal circulating levels of GAL-1, -3, and -13 increase as pregnancy progresses, and the levels of GAL-9 are nearly three times higher than nonpregnant levels at 8 weeks of gestation and remain elevated until parturition (20–23). Alternatively, dysregulated, altered, or insufficient levels of GAL-1, -3, -9, and -13 have been associated with pregnancy pathologies including preeclampsia, intrauterine growth restriction, preterm birth, and pregnancy loss (2, 20). GAL-9, a "tandem-repeat type" galectin, is structurally characterized by the presence of two different carbohydrate recognition domains (CRDs) with different sugar-binding affinities (24). During gestation, GAL-9 is expressed in the female reproductive tract and at the maternal-fetal interface (13, 15, 21). Decidual GAL-9 expression is disrupted in a mouse model of spontaneous abortion (17), indicating its significance in successful pregnancy. However, GAL-9 interactions with T-cell immunoglobulin mucin-3 (Tim-3) and CD44 receptors can have diverse effects depending on cell type-specific expression (8, 25, 26). Tim-3 is linked to T-cell exhaustion and tolerance, mediating apoptosis of Th1 and Th17 cells upon interaction with GAL-9 (27, 28). Conversely, GAL-9 also promotes inflammation by binding to Tim-3 in monocytes, dendritic cells, and macrophages. Notably, Tim-3 expression is

‡ These authors contributed equally to this work.
* For correspondence: Gabriela Dveksler, gabriela.dveksler@usuhs.edu.

upregulated on monocytes in pregnant compared to nonpregnant women (8, 29, 30). CD44 is an adhesion molecule that was shown to interact with murine GAL-9 and transforming growth factor (TGF)-βRI resulting in an increase in induced Tregs (iTregs) stability and function (9, 31).

Trophoblast cells of species with hemochorial-type placentation secrete pregnancy-specific glycoproteins (PSGs) into the maternal circulation (32). PSGs are members of the immunoglobulin superfamily and are closely related to the predominantly membrane-bound carcinoembryonic antigen-related cell adhesion molecules. As pregnancy progresses, the circulating levels of human PSGs in maternal serum reach levels greater than 100 μg/ml at full term (33–35). In humans, the PSG family comprises 10 members (PSG1-11, with PSG10 being a pseudogene), while mice possess a larger family with 17 members (Psg16-Psg32) (36, 37). There is evidence of rapid evolution of the *PSG* loci, characterized by differences in gene copy number, gene content, and nonconservative amino acid substitutions within ORFs (38–40). However, despite this genetic and structural diversity, both mouse and human PSGs retain conserved functions across species (41–46).

Using glycoproteomic studies, we previously showed that PSG1, one of the highest expressed members of the family throughout pregnancy, is heavily glycosylated with complex glycans containing poly-N-acetyl-lactosamine (LacNAc) elongated moieties that often serve as ligands for galectins (40, 41, 47). In addition, we demonstrated that GAL-1 binds to PSG1 in a carbohydrate-dependent manner and that the interaction of PSG1 and GAL-1 protects GAL-1 from inactivation due to oxidation (47, 48). However, whether other members of the galectin family found in the circulation of pregnant women interact with PSGs, and if murine PSGs interact with galectins, remains unknown.

Herein, we characterized the potential interaction between PSG1 and members of the human galectin family, including GAL-3, GAL-7, GAL-9, and GAL-13. We observed that PSG1 does not bind to all galectins tested. Of the galectins that bound to PSG1 (GAL-1, GAL-3, and GAL-9), GAL-9 presented the highest apparent affinity and the GAL-9-PSG1 interaction was carbohydrate-dependent. Therefore, we further characterized the ability of PSG1 to regulate GAL-9 responses in monocytes, macrophages, and T-cells and determined whether PSG1 binds to both GAL-9 CRDs. In addition, we compared the affinity of the interaction between GAL-9 and PSG1 to the other well-characterized GAL-9 ligands in these cells, Tim-3 and CD44. We found that murine Psg23, one of the highest expressed members of the murine PSG family (49), binds to murine GAL-9 and GAL-3, reinforcing the notion of conservation of function between members of the human and murine PSG families.

Results

Characterization of the binding of PSG1 to different members of the galectin family

Using surface plasmon resonance (SPR), we assessed the binding of GAL-3, GAL-7, GAL-9, and GAL-13 to recombinant and native PSG1 and compared the binding of these galectins to the previously identified PSG1 ligand, GAL-1 (47) (Fig. 1, *A* and *B*). We consecutively injected the different galectins at 1 μM over a PSG1-coated surface. However, we found that GAL-9 had to be injected at a lower concentration due to its increased binding to PSG1, compared to the other galectins (Fig. 1, *A* and *B*). As previously reported, PSG1 bound to GAL-1. Additionally, we observed that PSG1 binds to 1 μM GAL-3 and 0.1 μM GAL-9, and that the PSG1-GAL-9 interaction seemed to present the highest apparent affinity (Fig. 1*A*). On the other hand, we did not observe binding of 1 μM GAL-7 or GAL-13 to PSG1 (Fig. 1, *A* and *B*). The interaction of GAL-9 with PSG1 was further confirmed by ELISA (Fig. 1*C*). To determine whether the interaction between PSG1 and GAL-9 is carbohydrate-dependent, we used PNGase F to remove the complex N-glycans on PSG1. We observed a significant decrease in binding between the PNGase F-treated PSG1 and GAL-9 when compared to the untreated protein (Fig. 1*C*).

PSG1 has four immunoglobulin G (IgG)-like domains; three (N-, A1-, and A2) of the four domains are decorated by N-linked glycans (47). We determined that the binding of PSG1 to GAL-9 is mediated primarily by the glycans in the -N, and -A2 domains, as the binding was inhibited following treatment of these domains with PNGase F compared to the untreated proteins (Fig. 1*D*). Next, we defined the kinetics and affinity of the interaction between GAL-9 and PSG1 (Fig. 1, *E* and *F*). The calculated affinity of the interaction of GAL-9 for native and recombinant PSG1 was quite similar, with an estimated apparent KD of 21 and 40 nM, respectively (Tables 1 and 2). GAL-9 is composed of two CRDs, designated as the N-terminal CRD (GAL-9N) and the C-terminal CRD (GAL-9C). The linker peptide of certain GAL-9 splice variants can be cleaved by thrombin resulting in the separation of both GAL-9 CRDs (50). Interestingly, the two CRDs have similar albeit not identical specificities for glycans, and distinct activities have been proposed for these proteins as modulators of innate and adaptive immune cells (51–53). To determine if both GAL-9 CRDs bind to PSG1, we generated each CRD individually and performed binding studies. We observed that both domains of GAL-9 bound to PSG1 albeit with lower affinity than the full-length GAL-9 (Fig. 1*G*) and that the GAL-9 N-CRD domain binds with lower affinity to PSG1 than the GAL-9 C-CRD domain (Fig. 1, *H* and *I*).

Two well-characterized GAL-9 ligands in immune cells include Tim-3 and CD44 (8, 9, 54). The high-affinity binding of PSG1 to GAL-9 and its high concentration in maternal circulation suggests that PSG1 could compete with Tim-3 and CD44 for GAL-9 binding. Therefore, we assessed the kinetics of the interaction between GAL-9 and CD44 (Fig. 2*A*) and GAL-9 and Tim-3 (Fig. 2*B*). The calculated apparent affinity of the interaction of recombinant GAL-9 and Tim-3 and of GAL-9 and CD44 were very similar to the calculated affinity of the interaction between PSG1 and GAL-9 (Table 2). We carried out competition assays in which increasing concentrations of PSG1 were preincubated with a fixed concentration of GAL-9. These preparations were injected onto a chip with

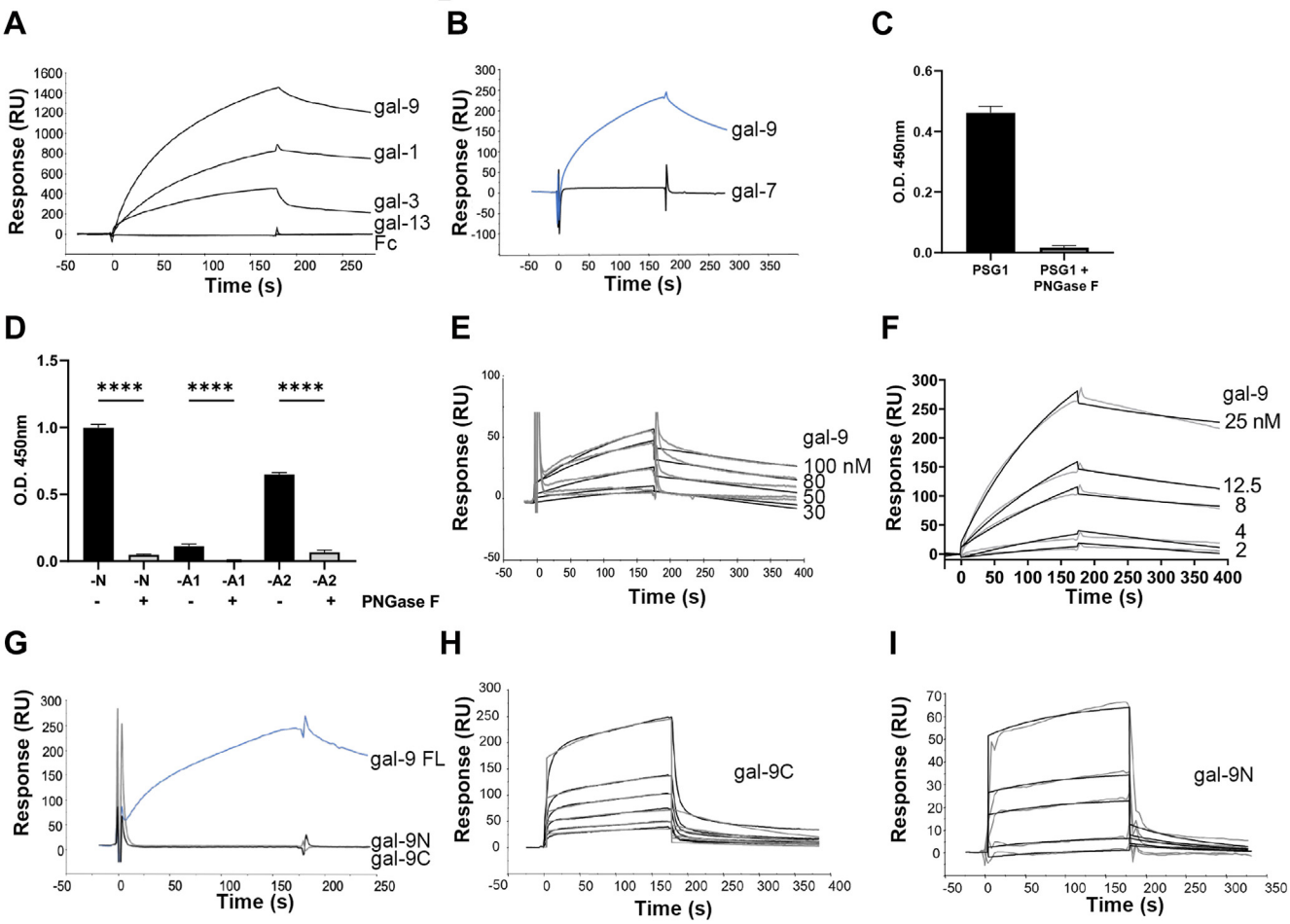

Figure 1. PSG1 interacts with GAL-9. *A*, SPR sensorgrams of the interaction of PSG1 with 0.1 μM GAL-9, 1 μM GAL-13, GAL-3, and GAL-1 and Fc as a negative control. A fixed concentration of each galectin was injected during 3 min over a CM5 biosensor with immobilized recombinant PSG1. *B*, sensorgrams of the interaction of PSG1 with 1 μM GAL-7 and 25 nM GAL-9. Galectins were injected during 3 min over a CM5 biosensor with immobilized recombinant PSG1. *C*, binding of 2 μg/ml of Fc-tagged recombinant PSG1N-Fc, PSG1A1-Fc, PSG1A2-Fc untreated or treated with PNGase F to GAL-9 coated wells. *D*, binding of 8 μg/ml of Fc-tagged recombinant PSG1 untreated or treated with PNGase F to GAL-9 coated wells. *E*, sensorgrams of the interaction of GAL-9 with native PSG1. Serial dilutions of GAL-9 ranging from 30 to 100 nM were injected during 3 min over a CM5 biosensor chip with immobilized native PSG1. *F*, sensorgrams of the interaction of GAL-9 with recombinant PSG1. Serial dilutions of GAL-9 ranging from 2 to 25 nM were injected during 3 min over a CM5 biosensor chip with immobilized native PSG1. *G*, SPR sensorgram showing the interaction of 25 nM of full-Length GAL-9 (FL), GAL-9C or GAL-9N domains were injected over a CM5 biosensor chip with immobilized PSG1. *H*, sensorgrams of the interaction of GAL-9C with recombinant PSG1. Serial dilutions of GAL-9C ranging from 200 nM to 2 μM were injected over a CM5 biosensor chip with immobilized native PSG1. *I*, sensorgrams of the interaction of GAL-9 N domain with recombinant PSG1. Serial dilutions of GAL-9 ranging from 200 nM to 10 μM were injected over a CM5 biosensor chip with immobilized native PSG1. In *E*, *F*, *H*, and *I*, SPR sensorgrams for each protein concentration are shown as *gray lines*, while the fitted data are shown as *black lines*. GAL-9, galectin 9; PSG, pregnancy-specific glycoprotein; SPR, surface plasmon resonance.

immobilized CD44 or Tim-3. As the concentration of PSG1 increased, we observed lower binding of GAL-9 to CD44 (Fig. 2*C*) and Tim-3 (Fig. 2*D*). These results indicate that PSG1 can compete the binding of GAL-9 to Tim-3 and CD44. We used PSG1 generated in GnTI$^-$ cells as control which was unable to compete the GAL-9 binding to Tim-3 or CD44 due to the absence of complex N-linked glycans (Fig. 2*E*).

PSG1 inhibits the GAL-9 mediated induction of TNF-α in human monocytes and a murine macrophage cell line

As previously reported for PSG1, serum GAL-9 levels increase in pregnant women as pregnancy progresses (21). Interestingly, GAL-9 has been shown to increase secretion of the inflammatory cytokine tumor necrosis factor alpha (TNF-α) in monocytes in a Tim-3-dependent manner (54). Tim-3 is

Table 1
Kinetics constants and apparent affinity of the interaction of full-length (FL) and single domains of GAL-9 with recombinant PSG1

PSG1	ka M^{-1} s^1 (mean ± SD)	kd s^{-1} (mean ± SD)	Rmax RU (mean ± SD)	Apparent KD M	Chi^2
GAL-9	(7.24 ± 0.08) × 10^4	(1.56 ± 0.2) × 10^{-3}	314 ± 28.7	2.16 × 10^{-8}	5.26
GAL-9C	(2.43 ± 0.08) × 10^3	(4.15 ± 0.04) × 10^{-3}	215 ± 5.8	1.70 × 10^{-6}	2.41
GAL-9N	(1.84 ± 0.11) × 10^0	(1.06 ± 0.09) × 10^{-2}	2110 ± 1250	5.78 × 10^{-3}	1.78

Table 2
Kinetics constants and apparent affinity of the interaction of CD44, Tim-3 and native PSG1, and recombinant Psg23 with full-length (FL) GAL-9

GAL-9 FL	ka M^{-1} s^{-1} (mean ± SD)	kd s^{-1} (mean ± SD)	Rmax RU (mean ± SD)	Apparent KD M	Chi^2
CD44	$(1.43 \pm 0.04) \times 10^5$	$(1.50 \pm 0.016) \times 10^{-3}$	956 ± 22.2	1.05×10^{-8}	23.8
Tim-3	$(1.7 \pm 0.9) \times 10^5$	$(3.3 \pm 0.1) \times 10^{-3}$	214 ± 11.1	2.67×10^{-8}	5
Native PSG1	$(3.9 \pm 0.3) \times 10^4$	$(1.6 \pm 0.2) \times 10^{-3}$	105 ± 6.9	4.03×10^{-8}	2.7
rPsg23	$(2.79 \pm 0.06) \times 10^6$	$(6.35 \pm 0.05) \times 10^{-3}$	0.044 ± 0.003	2.28×10^{-9}	0.89

primarily expressed in monocytes in the peripheral blood of pregnant women, with significantly higher levels observed in preeclampsia patients compared to normal pregnant women (21, 55). Therefore, we investigated the functional significance of the PSG1 and GAL-9 interaction in relation to Tim-3 engagement.

Consistent with the role of Tim-3 in response to GAL-9 in monocytes or macrophages, we did not observe an increase in TNF-α secretion in the monocyte-like cell line THP-1 treated with GAL-9. Flow cytometry confirmed that these cells do not express Tim-3 (data not shown), supporting these data (56). Using monocytes isolated from several donors, we showed that PSG1 reduces the GAL-9-mediated induction of TNF-α (Fig. 3*A*). We also observed that GAL-9 induced TNF-α in the murine macrophage cell line RAW 264.7 that expresses Tim-3, and that this increase was inhibited by coincubation of GAL-9 with PSG1 prior to cell treatment (Fig. 3*B*). These data suggest that PSG1 inhibits the ability of GAL-9 to increase TNF-α secretion in human monocytes or murine RAW 264.7 macrophages. Furthermore, GAL-9 treatment of RAW-blue reporter cells did not activate the NF-kB and AP-1 transcription factors at the concentrations where we observed increased TNF-α levels, in contrast to that observed with our positive control lipopolysaccharide (LPS) (Fig. 3*C*), indicating distinct differences in the signaling pathways triggered by these two inducers of TNF-α.

GAL-9 induced apoptosis of Jurkat and primary CD4⁺ T cells is not inhibited by PSG1

GAL-9 modulates the adaptive immune response by mediating T cell death or suppression on activated $CD4^+$ Th1 and Th17 cells, and in CD8+ T cells (8, 57, 58). In addition, GAL-9 induces apoptosis in several leukemic T cell lines, including Jurkat cells, which lack Tim-3 expression unless treated with phorbol myristate acetate (8, 59–61). We studied whether coadministration of GAL-9 and PSG1 affects the ability of GAL-9 to mediate apoptosis in Jurkat cells. PSG1 at a concentration as high as 50 μg/ml did not inhibit the GAL-9-mediated apoptosis (Fig. 4*A*). We also evaluated whether PSG1 would have an effect in the GAL-9-mediated apoptosis of primary $CD4^+$ T cells. Similarly to what we observed in the Jurkat T cell line, the interaction between PSG1 and GAL-9 did not affect the ability of GAL-9 to induce apoptosis in

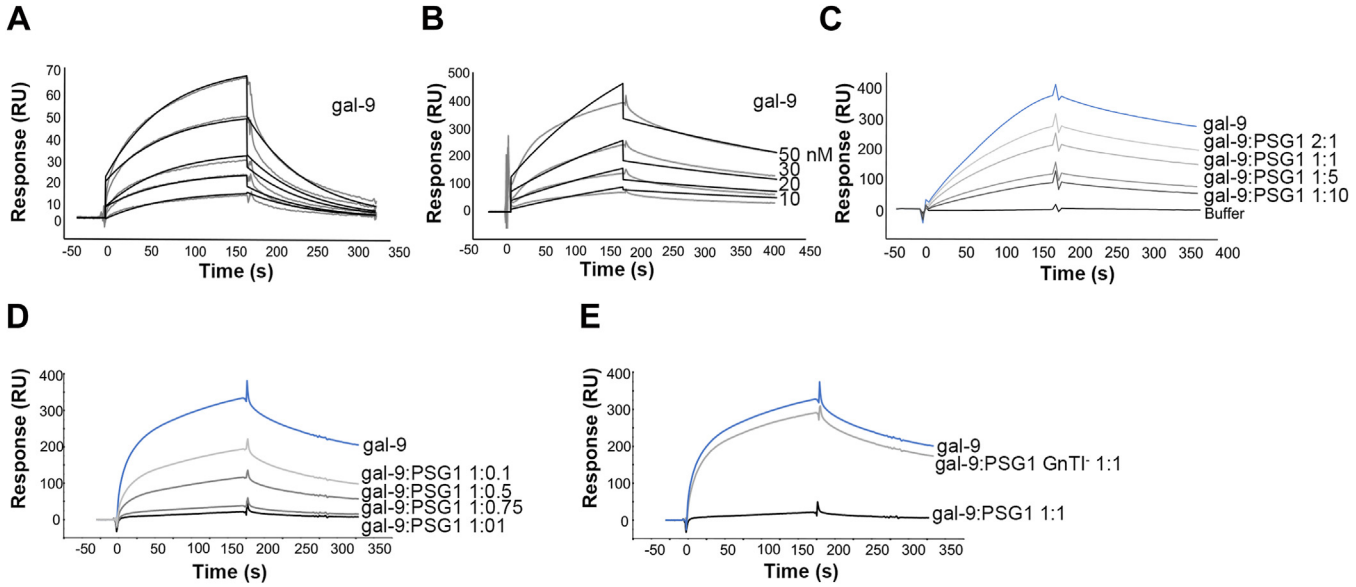

Figure 2. PSG1 can inhibit the binding of GAL-9 to Tim-3 and CD44. *A*, sensorgrams of the interaction of GAL-9 with CD44. Serial dilutions of GAL-9 ranging from 2 to 25 nM were injected during 3 min over a CM5 biosensor chip with immobilized native CD44. SPR sensorgrams for each protein concentration are shown as *gray lines* while the fitted data are shown as *black lines*. *B*, sensorgrams of the interaction of GAL-9 with Tim-3 represented as in A. Serial dilutions of GAL-9 ranging from 10 to 50 nM were injected during 3 min over a CM5 biosensor chip with immobilized native Tim-3. *C*, sensorgrams of the interaction of 25 nM GAL-9 preincubated with recombinant PSG1 injected over a biosurface of immobilized CD44. GAL-9 and PSG1 were preincubated at the indicated molar ratio and injected during 3 min over a CM5 biosensor chip with immobilized recombinant CD44. *D*, sensorgrams of the interaction of 25 nM GAL-9 preincubated with recombinant PSG1 at the indicated molar ratio injected over a biosurface with immobilized Tim-3. *E*, SPR sensorgram showing the interaction of 25 nM GAL-9 or preincubated with 25 nM PSG1 produced in CHOK1 (PSG1) or GnTI-deficient cells (PSG1GnTI⁻) before injection over a biosurface of immobilized TIM3. GAL-9, galectin 9; PSG, pregnancy-specific glycoprotein; SPR, surface plasmon resonance; Tim-3, T-cell immunoglobulin mucin-3.

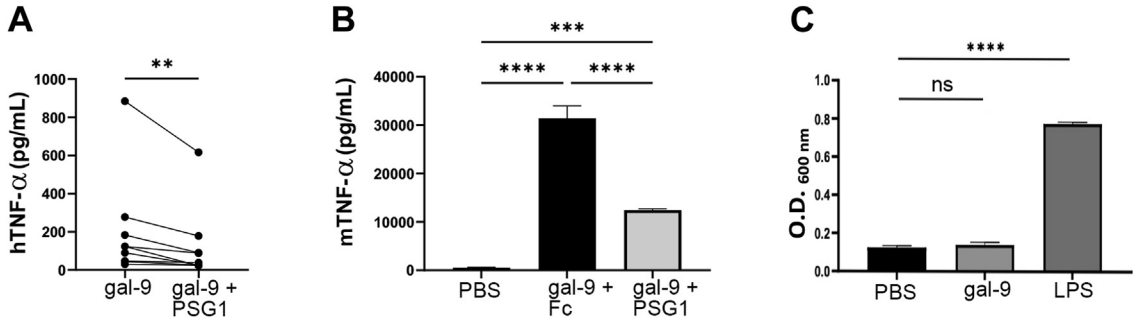

Figure 3. PSG1 inhibits the GAL-9 mediated induction of TNF-α in human monocytes and RAW 264.7 cells. *A*, human monocytes were treated in duplicate or triplicate with GAL-9 (40–70 nM) alone or in combination with PSG1 (40 μg/ml). TNF-α was measure in supernatants at 48 post-treatment. *B*, RAW 264.7 cells were treated in triplicate with GAL-9 (20 nM) alone or in combination with PSG1 (40 μg/ml) or the Fc control. mTNF-α was measured in supernatants at 20 h post treatment. *C*, RAW-Blue reporter cells were treated with PBS, GAL-9 (3 μg/ml), or LPS (1 ng/ml) and the levels of SEAP in the supernatant was measured 18 h post treatment using the QUANTI-Blue reagent. GAL-9, galectin 9; LPS, lipopolysaccharide; PSG, pregnancy-specific glycoprotein; SEAP, secreted embryonic alkaline phosphatase; TNF-α, tumor necrosis factor alpha.

anti-CD3/CD28 stimulated primary human $CD4^+$ T cells, including naïve $CD4^+$ T cells (Fig. 4*B*, and data not shown). Furthermore, we examined whether the individual CRDs of GAL-9 could induce apoptosis. We found that neither the GAL-9N nor the GAL-9C CRDs induced apoptosis in primary $CD4^+$ T cells (Fig. 4, *C–E*), suggesting that full-length GAL-9 is required to trigger apoptosis in Jurkat and primary human $CD4^+$ T cells.

GAL-9 did not induce conversion of $CD4^+$ T cells into $Foxp3^+$ cells in the presence or absence of TGF-β

Wu *et al.* reported that mouse GAL-9 modestly promotes induction of murine Foxp3-expressing iTregs, and that the interaction with CD44 enhances the stability and function of these cells (9). On the other hand, the addition of both human GAL-9 and TGF-β was needed to see substantial induction of iTregs (9, 62). We explored whether the addition of both PSG1 and human GAL-9, in the presence or absence of recombinant TGF-β1, would increase the number of human $CD4^+$ T cells expressing $Foxp3^+$. We observed that in the absence of TGF-β, GAL-9 did not induce the conversion of naïve $CD4^+$ T cells into $Foxp3^+$ cells (Fig. S1*A*). As expected, the addition of 5 ng/μl TGF-β to naïve $CD4^+$ T cells, which were activated with anti-CD3/CD28 beads and interleukin-2 (IL-2), increased the frequency of $Foxp3^+$ cells (Fig. S1*B*). However, we observed a trend in the increase of Foxp3+ T cells (albeit not statistically significant) when GAL-9 and TGF-β1 were added under the same experimental conditions *in vitro*. Furthermore, we observed that increasing the concentration of GAL-9 from 20 to 40 nM led to a decrease in cell viability (data not shown). When treating the cells with a combination of PSG1, GAL-9, and TGF-β1, we observed no significant change in the frequency of $Foxp3^+$ cells, although the cell viability remained above 70% (Fig. S1*B*), suggesting that human GAL-9 with or without TGF-β1 does not convert human $CD4^+$ T cells into $Foxp3^+$ cells.

Recombinant Psg23 directly binds to GAL-9 in a glycan-specific manner

Like human PSGs, murine Psgs contain multiple potential N-linked glycosylation sites, although their domain structure differs. Typically, murine Psgs consist of three Ig variable-like Ig domains, referred to as N domains, followed by an A-domain (46). Psg23 exhibits an N1-N2-N3-A domain arrangement, featuring a total of seven potential N-linked glycosylation sites across all domains except the A-domain (43). Murine pregnancy models are frequently used and have been valuable in replicating many immunological features observed in human pregnancy pathologies (63). To investigate the conservation of ligands between human and murine Psgs, we generated recombinant full-length Psg23 and assessed its binding to murine GAL-1, GAL-3, and GAL-9. Additionally, we evaluated the potential binding of rPsg23 to human GAL-7, since its mouse counterpart is not commercially available (Fig. 5*A*). We did not study the potential binding of GAL-13 to Psg23 because this galectin is only expressed in anthropoid primates (18). Consistent with our observations for PSG1, GAL-3, and GAL-9 bound to Psg23, with GAL-9 showing the highest affinity for Psg23. However, we did not detect binding between Psg23 and murine GAL-1 (Fig. 5*A*), even when using recombinant murine GAL-1 commercially available from two different vendors. Next, we calculated the apparent affinity of the interaction of Psg23 with GAL-9 (Fig. 5*B*). This interaction was confirmed to be carbohydrate-mediated, as binding was inhibited in the presence of lactose, an inhibitor of galectin–glycan interactions, but not in the presence of sucrose (Fig. 5*C*).

Discussion

This study provides evidence that PSG1 interacts with GAL-9, GAL-1, and GAL-3, but not with GAL-7 or GAL-13. PSG1 presents a higher affinity for GAL-9 compared to GAL-1 and GAL-3 (47). Furthermore, we observed that the interaction between GAL-9 and PSG1 is sugar-dependent, similar to that reported for the GAL-9 interaction with Tim-3 (60, 64). Moreover, we found that PSG1 competes with Tim-3 for interaction with GAL-9. Notably, mouse Psg23 also interacts with mouse GAL-9, underscoring the functional conservation between murine and human PSGs.

GAL-9 is involved in various biological processes, including chemoattraction, cell aggregation, cell proliferation, cell

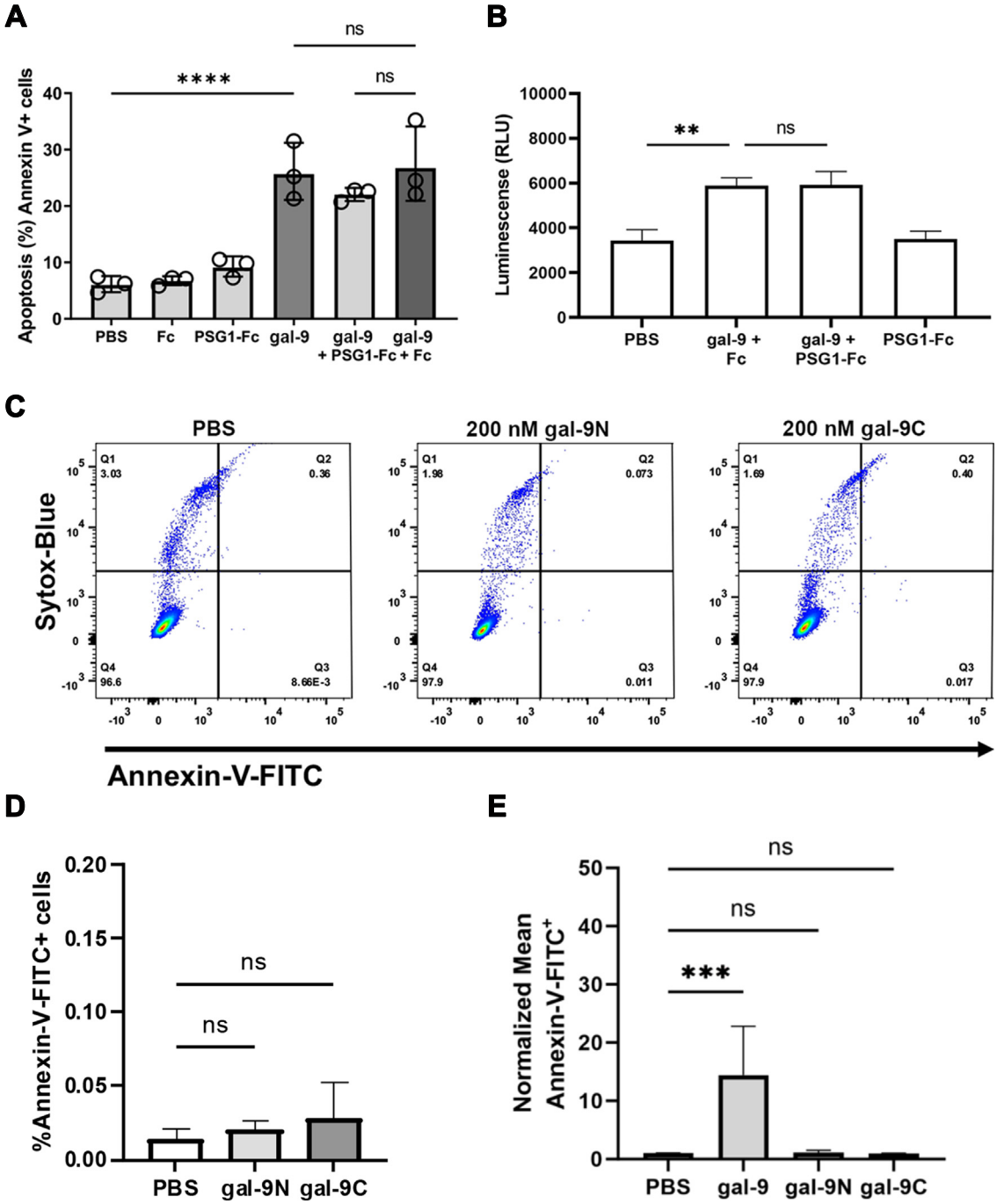

Figure 4. PSG1 does not inhibit GAL-9-induced apoptosis in Jurkat cells. *A*, GAL-9 induces apoptosis in Jurkat cells at 200 nM. PSG1-Fc or the Fc control at 0.7 μM (50 μg/ml) were preincubated with gal-9 and added to Jurkat cells. After 24 h, cells were stained with annexin-V-FITC to assess apoptosis. *B*, *in vivo* cell viability monitoring using RealTime-Glo annexin-V apoptosis and necrosis assay were performed to show apoptosis in primary T cells. PSG1 or Fc control at 0.7 μM were preincubated with GAL-9 and added to primary T cells (30,000 cells per well) isolated from PBMCs from four different donors. RealTIME-Glo was added at seeding and readings were taken 24 h after incubation. All measurements were performed in triplicate and data were expressed as mean ± standard deviation (SD). *C*, Jurkat cells were incubated with single domains of GAL-9 (GAL-9N or GAL-9C) at 200 nM. After 24 h, the percentage of apoptotic cell death was assessed by flow cytometry analysis using annexin-V-FITC and SYTOX Blue. *D*, percentage of annexin-V-FITC positive cells or (*E*) normalized annexin-V-FITC$^+$ fluorescence intensity from three independent experiments (n = 3) are presented as mean ± SD. Data were analyzed by one-way analysis of variance (ANOVA) followed by Dunnett's test. p value < 0.05 was considered statistically significant. FITC, fluorescein isothiocyanate; GAL-9, galectin 9; PBMC, peripheral blood mononuclear cell; PSG, pregnancy-specific glycoprotein.

survival, and immunomodulation of inflammation. These functions are mediated by its intracellular activities and/or the interaction with multiple cell surface receptors (65). Besides Tim-3 (8, 66, 67) and CD44 (9), GAL-9 binds to CD137 (also known as 4-1BB) (68), CD206 (69), protein disulfide isomerase (PDI) (69), lysosomal-associated membrane protein 2 (Lamp2) (70), bacterial LPS (71), VISTA (56), Dectin-1 (72), and PD-1 (60). The equilibrium constant for the interaction between

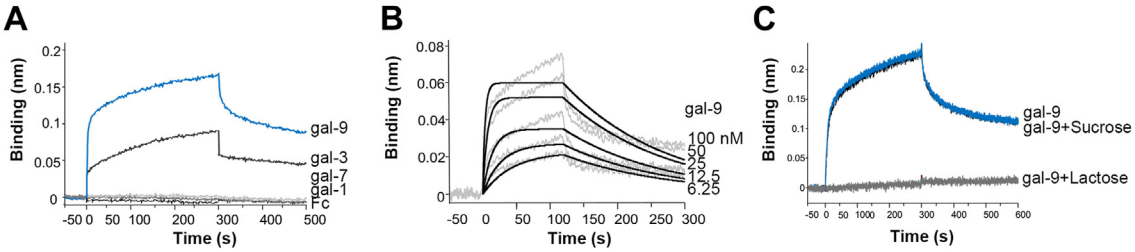

Figure 5. Recombinant mouse Psg23 (rPSG23) interacts with mouse GAL-3 and GAL-9. *A*, sensorgrams of the interaction of rPsg23 with 1 μM human GAL-7, 0.1 μM murine GAL-9, 1 μM murine GAL-3, GAL-1, or Fc (as negative control). *B*, sensorgrams of the interaction of murine GAL-9 with rPsg23 for kinetics calculations. Binding of serial dilutions of GAL-9 ranging from 6.25 to 100 nM to an AR2G biosensors with immobilized rPsg23. *C*, sensorgrams of the interaction of murine 0.1 μM GAL-9 with immobilized rPsg23 in the absence (*blue*) or presence of 1.5 μM of sucrose (*black*) or lactose (*gray*). AR2G, amine reactive second generation; GAL-9, galectin 9; PSG, pregnancy-specific glycoprotein.

GAL-9 and some of its ligands has been reported to be in the nanomolar range. Interestingly, the apparent affinity we estimated for the GAL-9 and PSG1 interaction is also in the nanomolar range (Fig. 1), suggesting that PSG1 may compete with several ligands for GAL-9 binding, as we show here for Tim-3 and CD44 (Fig. 2).

Additionally, we explored the potential role of PSG1 in GAL-9 induced proinflammatory cytokine production in three different cell types. We observed induction of TNF-α in human monocytes and RAW 264.7 cells using *Escherichia coli*-derived GAL-9 from R&D systems at concentrations up to 3 μg/ml (Fig. 3). However, this concentration was insufficient when using the HEK293-derived GAL-9 from R&D systems or BioLegend (data not shown). Differences in recombinant GAL-9 activity have been noted depending on its mode of production. For instance, HEK293-derived recombinant human GAL-9 binds with lower affinity to Tim-3 than the *E. coli*-derived recombinant protein as indicated in the product data sheet from R&D systems (Bio-Techne). It has also been proposed that GAL-9 obtained from cells may display higher activity compared to recombinant GAL-9 preparations, potentially necessitating lower concentrations of GAL-9 to observe its *in vivo* effects (56). In RAW-blue cells, we found that GAL-9 did not induce activation of NF-κB, a transcription factor involved in LPS- induced TNF-α secretion in myeloid cells. These data suggest TNF production induced by *E. coli*-derived GAL-9 is not induced by contaminating endotoxin. Rather, Matsuura *et al.* suggested that the induction of proinflammatory cytokines by GAL-9 is mediated through the activation of leucine zipper transcription factors NF-IL6 or AP-1 (73). Moreover, it was recently reported that the Tim-3 and GAL-9 interaction can activate mammalian target of rapamycin (mTORC) in myeloid leukemia cells (74).

The N-terminal and C-terminal CRDs of GAL-9 exhibit only 39% amino acid homology and display different oligosaccharide binding affinities, suggesting different roles for each CRD in mediating GAL-9 functions (53, 75, 76). Several studies have shown that GAL-9C exhibits greater antiproliferative and proapoptotic activities compared to GAL-9N, and that while full-length GAL-9 was more efficient, both CRDs retained the ability to induce TNF-α in dendritic cells (77, 78). However, our attempts to replicate these findings in monocytes and T cells using individual GAL-9 CRDs were unsuccessful, matching failed attempts by other groups (Fig. 4). This could be attributed to the use of monomeric *versus* dimeric CRDs and the concentrations tested, since the experiments conducted by Li *et al.* used dimeric Fc-tagged forms of the individual CRDs at significantly higher concentrations (53).

Murine GAL-9 was reported to promote Foxp3 expression during iTreg cell differentiation of murine $CD4^+$ T cells, although the concentration of GAL-9 used was not reported (9). In addition, during *in vitro* differentiation, GAL-9 alone induced a modest increase in Foxp3 expression in activated naïve $CD4^+$ T cells, while a substantial synergistic effect of GAL-9 with TGF-β in inducing Foxp3 expression was observed for both human naïve $CD4^+$ T and murine T cells (9, 62, 79). However, although we observed a slight increase in the percentage of $CD4^+$ $CD25^+$ $Foxp3^+$ cells, it did not reach statistical significance (Fig. 4*D*). Lv *et al.* reported that human GAL-9 purchased from ProSpec-Tany TechnoGene, Ltd, at different concentrations (up to 80 nM) when combined with TGF-β, induced the conversion of mouse naïve $CD4^+$ T cells into $Foxp3^+$ iTreg cells although the effect of GAL-9 was not dose-dependent (62). In our hands, we observed reduced cell viability (∼70%) with different source of GAL-9 at 80 nM relative to untreated cells, hindering us from testing higher concentrations. Yang *et al.* reported that similar to conventional $CD4^+$ T cells, human Treg cells are susceptible to GAL-9-induced cell death, suggesting that the ability of GAL-9 to induce apoptosis dominates its Treg promoting activity (60). Overall, in our hands, using human cells and human GAL-9, the coadministration of PSG1, GAL-9, and TGF-β1 did not increase the frequency of $Foxp3^+$ cells in comparison to GAL-9 and TGF-β1.

Based on our results, we propose that the interaction between PSG1 and GAL-9 may be beneficial during pregnancy by disrupting the binding of GAL-9 to Tim-3 in monocytes. This competitive disruption reduces GAL-9-induced secretion of the proinflammatory cytokine TNF-α, which has been shown to have detrimental effects in pregnancy (80, 81). On the other hand, PSG1 did not affect GAL-9-mediated apoptosis of primary $CD4^+$ T cells (or Jurkat T cells), which is mediated by an unknown GAL-9 receptor.

Several mechanisms have been proposed to explain how during pregnancy, the immune system shifts toward a

dominant Th2 immune response (82). For example, it has been shown that there is apoptosis of decidual Th1 cells mediated by GAL-1 (83). As GAL-9 is also present in the placenta, we posit that GAL-9 may induce apoptosis of Th1 cells to help establish a Th2-predominant phenotype. During uneventful pregnancies, in both the placenta and the maternal circulation, GAL-1 is the most abundant member of the galectin family, followed by GAL-3 and GAL-9, respectively (20, 22, 84). Differences in PSG1 affinity for galectins may be explained by the galectin dynamics during healthy gestation. PSG1 bound to GAL-9 with higher affinity than GAL-1, potentially because GAL-9 is less abundant at the maternal/fetal interface. Although we did not observe an interaction between GAL-7 and PSG1, it is important to point out that these two proteins do not have similar kinetics of expression during pregnancy; GAL-7 peak concentration is observed at gestation weeks 13 to 16, while the concentration of PSGs continually increase as pregnancy progresses (32, 84, 85). Although GAL-13, like GAL-1, belongs to the galectin prototype subtype, evolutionary and sugar-binding analyses revealed functional diversification in its CRD due to missense mutations that alter carbohydrate-binding specificity. For example, GAL-13 has less affinity for lactose and stronger affinity for mannose compared to other galectins. Therefore the absence of interaction between PSG1 and GAL-13 may be due to preferential binding affinity of GAL-13 for different beta-galactosides *versus* GAL-1, and for blood sugar antigens as evidenced by several studies (86–88). Importantly, we cannot exclude the possibility that PSG1 can bind to more than one type of galectin simultaneously *via* different glycans decorating the protein, resulting in multivalent interactions which are utilized by cells in a diverse range of cellular processes (89).

The difference in affinity between PSG1 and various galectins is likely relevant in the fine-tuning of physiological processes during pregnancy, regulated in a carbohydrate-dependent manner in which the concentration of the different players may be affected during pathological conditions or by genetic differences (2, 39). During gestation, GAL-9 levels have been reported to increase as early as 8 weeks of gestation in normal pregnancies compared to nonpregnant controls (21, 90). In a study involving 30 primigravida women, those carrying male fetuses had higher GAL-9 levels in circulation compared to those carrying females (21). Interestingly, we found that PSG1 concentrations were significantly lower in African American women diagnosed with preeclampsia compared to controls, but only when carrying a male fetus (35). These observations suggest that an abnormal balance of PSG1 and GAL-9 levels may be associated with pregnancy pathologies in a sex-dependent manner, as previously suggested for Tim-3 and GAL-9 (91).

Due to the ethical limitations in performing studies in pregnant women, several studies underscoring the importance of galectins in reproduction have been undertaken using mouse models. Given that murine Psg23 is one of the highest expressed murine Psgs (46, 47, 49, 92), we explored whether recombinant (rPsg23) can interact with murine galectins. Despite having different Ig domain arrangements, previous studies demonstrated that some members of the murine Psg family share functional conservation with human PSGs, including the ability to activate latent TGF-β1, induce endothelial tube formation, and bind to αIIbβ3 integrin in platelets (41–43, 45, 46, 93). Here, we showed that rPsg23 binds to GAL-9, adding GAL-9 to the list of conserved ligands for human and murine PSGs (Fig. 5). Interestingly, while we observed binding of human GAL-1 to rPsg23 (data not shown), rPsg23 failed to interact with murine GAL-1 from two different commercial sources, despite 88% shared sequence homology between murine and human GAL-1. Future studies are required to determine whether native murine Psgs bind to murine GAL-1, as glycans may differ between native and recombinant proteins.

The studies presented here suggest that specific changes in the PSG-glycan composition may affect some functions of these proteins. Indeed, placental tissues derived from women with early onset preeclampsia show evidence of endoplasmic reticulum stress, leading to synthesis and secretion of mis-glycosylated glycoproteins into the maternal circulation. One of the identified mis-glycosylated proteins was PSG5, meaning changes in PSG glycosylation could affect galectin binding (94). Characterization of the interaction between galectins and PSGs will allow for a better understanding of multiple biological processes influenced by these two protein families during pregnancy, including immunomodulation, angiogenesis, and trophoblast invasion.

Experimental procedures

Protein production and purification

Native PSG1 was obtained from serum of pregnant women as previously reported (47). Recombinant murine Psg23-myc-His (Psg23) (95) was generated by transient transfection of ExpiCHO cells (Thermo Fisher Scientific). Clarified supernatants collected 6 days posttransfection were bound to a HisTrap column (Cytiva) 10 mM imidazole and were eluted with 200 mM imidazole. The proteins eluted at 200 mM imidazole were buffer exchanged into PBS and concentrated using Amicon Ultra-15 10K molecular weight cutoff centrifugal filter units (Millipore) and further purified by gel filtration chromatography on a HiLoad 16/200 Superdex 200 column (Cytiva). The proteins which corresponded to the expected molecular weight were then further concentrated. PSG1 with the V5His tags was obtained by transient transfection of GnTI-deficient HEK293 cells and purified on a HisTrap and gel filtration column as previously described (47).

Proteins consisting of only the Fc tag, the entire coding region of PSG1, or individual domains fused to the Fc tag were generated by transfection of ExpiCHO cells following the standard protocol, and the supernatants were harvested when the cells were over 70% viable, in most cases 5 days post transfection. The Fc tag, consisting of the hinge region and CH2 and CH3 domains of the IgG1 heavy chain, was added to the proteins at the C terminus by cloning the specific complementary DNA in-frame into the pFUSE-IgG1-e3-Fc1 vector (InvivoGen). Fc-tagged proteins were purified from cell

supernatants using protein A columns as previously described (96).

The GAL-9 N- and C-CRDs were generated in *E. coli* strain Rosetta 2 (Merck Millipore) and purified from the supernatant by affinity chromatography using lactosyl-sepharose as previously described (76). The proteins were passed through an EndoTrap column (Lionex) to remove potential traces of endotoxin that can induce TNF-α in monocytes. All recombinant proteins generated for these studies were checked for purity by separation on 4 to 20% NuPAGE Bis-Tris gels followed by staining of the gel with GelCode Blue (Thermo Fisher Scientific) and were quantitated against bovine serum albumin (BSA) standards run on the same gel.

Recombinant human GAL-1 was purchased from PeproTech (catalog# 450–39). Recombinant human GAL-7 was purchased from R&D systems (catalog# 1339-GA/CF). Recombinant GAL-13 was purchased from Prospec (catalog# CYT-004). Recombinant human GAL-9 was purchased from different suppliers including R&D systems (catalog# 2045-GA and 9064-GA), BioLegend (catalog# 557306), and MyBioSource(catalog# MBS2097223). Recombinant mouse GAL-1 (catalog# 1245-GA/CF) and GAL-9 (catalog# 3535-GA/CF) were purchased from R&D systems and mouse GAL-3 (catalog# ABIN 7274752) and mouse GAL-1 with an Fc tag (catalog# ABIN7274695) were purchased from antibodies-online.com. Recombinant human Tim-3-Fc was purchased from BioLegend (catalog# 759904). Recombinant human CD44 (catalog# 3660-CD) and TGF-β were purchased from R&D systems (catalog# 246-LP/CF).

Cell culture

THP-1 and Jurkat cells, both obtained from the American Type Culture Collection, were maintained in RPMI-1640 medium (Thermo Fisher Scientific) containing 10% heat-inactivated (HI) fetal bovine serum (FBS), 1 mM sodium pyruvate, 4.5-g/L glucose. RAW264.7 was obtained from the American Type Culture Collection and was cultured and maintained in Dulbecco's modified Eagle's medium (Thermo Fisher Scientific) containing 10% HI FBS, 1% penicillin–streptomycin, and 100 μg/ml normocin (InvivoGen). The RAW-blue reporter cell line was obtained from InvivoGen (catalog# raw-sp) and cultured and maintained as recommended by the vendor. Peripheral blood mononuclear cells (PBMCs) were acquired from anonymous de-identified healthy human donors at the National Institutes of Health Blood Bank, with access kindly provided by Dr Michael Lenardo. All National Institutes of Health Blood Bank donors provide informed consent to give blood for research purposes. PBMCs were separated using a Ficoll separation gradient. Following centrifugation, the PBMC layer was extracted and washed twice using PBS. Naïve $CD4^+$ T cells were isolated *via* negative selection using the EasySep Human Naïve CD4+ T Cell Isolation Kit (STEMCELL Technologies, catalog#19555) according to the manufacturer's instructions and were maintained in RPMI-1640 medium containing 10% FBS, 1-mM sodium pyruvate, and 4.5 g/L glucose. Cells were activated with the Enceed human T cell activation anti-CD3/anti-CD28 beads (GenScript, catalog#L00899) and human IL-2 (PeproTech, catalog#200–02). Human monocytes were isolated from PBMCs based on their expression of CD14 using the EasySep Human Monocyte Isolation Kit (STEMCELL Technologies, catalog# 19359) and maintained in macrophage serum-free media (Thermo Fisher Scientific catalog# 12065–074). All cells were maintained in a humidified atmosphere of 5% CO_2 and 95% air at 37 °C.

PNGase F treatment

Between 10 and 20 μg of Fc-tagged Psg23 and PSG1N, PSG1A1, and PSG1A2 domains or the Fc only control protein were incubated with Remove-iT PNGAse F (1 μl or 225 units/reaction) for 2 h at 37 °C as recommended by the manufacturer (New England Biolabs, catalog#P0706s). Once the reaction ended, the enzyme was removed from the solution using chitin magnetic beads per the manufacturer instructions (New England Biolabs). The proteins before and after PNGase F-treatment were separated side by side on 4 to 20% NuPAGE Bis-Tris gels followed by staining with GelCode Blue for protein visualization and quantitation against BSA standards.

Surface plasmon resonance and biolayer interferometry experiments

SPR experiments were performed in a Biacore 3000 instrument (GE HealthCare) at a flow rate of 10 μl/min and 25 °C using HBS-EP (0.01 M Hepes pH 7.4, 0.15 M NaCl, 3 mM EDTA, and 0.005% v/v surfactant P20) as running buffer. Purified recombinant PSG1, Psg23, or native PSG1 were immobilized onto a CM5 sensor chip (Cytiva) in 10 mM sodium acetate pH 4.0 using standard amine coupling chemistry. A control surface where no protein was immobilized was used as control to correct for background and potential nonspecific binding. GAL-9 (R&D, catalog# 2045-GA from R&D) was injected over a range of concentrations (100 μM to 125 nM) for 180 s followed by a 240 s dissociation period. To regenerate the surface after each GAL-9 injection, a solution containing 1 M NaCl and 20 mM NaOH in HBS-EP buffer was injected for 30 s. Real-time data were analyzed using the BIAevaluation 4.1 software (GE HealthCare; https://biaevaluation.software.informer.com/4.1/#google_vignette), and kinetic profiles were fitted using a global 1:1 binding algorithm to estimate the association (ka) and dissociation (kd) constant, and the apparent affinity (KD) of the interaction. To calculate kinetics of the interaction of GAL-9 with Tim-3 and CD44, Tim-3 or CD44 in 10 mM sodium acetate pH 4.0 was immobilized by amine coupling on independent surfaces of a CM5 chip. A control surface where no protein was immobilized was used to correct for background and potential nonspecific binding, and serial dilutions of GAL-9 were injected over these surfaces. For competition experiments, different concentrations of PSG1 were incubated with GAL-9 as indicated in the figures in HBS-EP buffer for 30 min at room temperature (RT). As a control, GAL-9 at the same concentration and buffer was incubated for 30 min at RT. These GAL-9-PSG1 preparations were injected

over an SPR biosurface with immobilized recombinant Tim-3 or CD44 using the same flow, running buffer, temperature, and regeneration conditions described above. PSG1 produced in CHO-K1, ExpiCHO, or HEK293 GnTI-deficient cells were immobilized in independent biosurfaces of a CM5 sensor chip as indicated before for recombinant or native PSG1. GAL-9 was injected simultaneously over the three different surfaces, and a control surface with no protein immobilized. Real-time sensorgrams were aligned using the BIAevaluation 4.1 software.

Biolayer interferometry experiments were performed in an Octet R8 (Sartorius Corporation). Psg23 diluted at 40 μg/ml in sodium acetate pH 4.0 was immobilized on amine reactive second generation biosensors using standard amine coupling chemistry and following the manufacturer instructions. HBS-EP buffer was used for baseline recordings, the dissociation steps, and to dilute the analytes (murine GAL-9, GAL-3, GAL-1, human GAL-7, and Fc control). For kinetic experiments, Psg23 was associated for 120 s with increasing concentration of GAL-9 ranging from 200 to 6.25 nM and left to dissociate in HBS-EP buffer for 180 s. For competition assays, 0.1 μM GAL-9 was diluted in HBS-EP without or with the addition of either 0.5 to 1.5 μM sucrose or lactose before binding to Psg23. All data analysis was performed with the Octet Analysis Studio (https://www.sartorius.com/en/products/biolayer-interferometry/octet-systems-software).

ELISAs

The direct interaction of PSG1 with human GAL-9 was determined by ELISA. Wells of a 96-well plate were coated with GAL-9 (8 μg/ml) in PBS overnight at 4 °C. The coated wells were washed with PBS, 0.05% Tween-20, and the residual binding sites were blocked with 3% BSA in PBS. After washing, 2 μg/ml of native PSG1 was added for an overnight incubation at 4 °C. Bound PSG1 was detected with biotin-labeled anti-PSG MAb#4 (32) followed by streptavidin-HRP (BD Biosciences).

Cell treatments

Monocytes were seeded at 3.5 to 4 x 10E5 cells per well in macrophage serum-free media in a 96-well plate in 100 μl and treated in triplicate wells with 1.5, 2.5, or 3 μg/ml of GAL-9 (R&D, catalog# 2045-GA) or PBS for 24 h (final volume = 125 μl/well) to determine the concentration of GAL-9 required for each donor to observe induction of TNF-α. For treatments with GAL-9 (the concentration was chosen based on the response of the particular donor) and PSG1-Fc (*versus* Fc only control), proteins were coincubated in 25 μl for 1 h at 37 °C prior to the addition to monocytes seeded as described above. Cell supernatants were collected 24 h after treatment and stored at −20 °C. Human TNF cytokine levels were determined by ELISA using the Human TNF-alpha DuoSet ELISA kit according to the manufacturer's instructions (Catalog# DY210–05). RAW 264.7 cells were seeded in triplicate for each treatment on a 96-well plate at 1.8 × 10E6 cells/ml, in 100 μl per well for 3 h. Treatments were added in 50 μl for a total volume of 150 μl/well for 20 h. Mouse TNF-α cytokine levels were determined by ELISA using mouse TNF-alpha DuoSet ELISA kit (R&D, catalog#DY410–05) according to the manufacturer's instructions.

RAW 264.7 macrophages carrying a secreted embryonic alkaline phosphatase (SEAP) reporter construct inducible by the NF-κB- and AP-1 transcription factors (RAW-Blue, InvivoGen) were scraped from the flask and resuspended in RAW-Blue test media (Dulbecco's modified Eagle's medium, 10% HI FBS, 100 μg/ml normocin and 2 mM L-glutamine). Cells were then plated at 1 × 10E5 cells per well in a 96-well plate in a 180 μl volume in triplicate wells for each treatment. GAL-9 and ultrapure LPS.B5 (InvivoGen) at the concentrations indicated were added for a final volume of 200 μl. After an 18-h incubation, secreted embryonic alkaline phosphatase was detected in the supernatants using the QUANTI-Blue detection medium according to manufacturer recommendations (InvivoGen). The plate was read at 600 nm in a GloMax plate reader (Promega).

Apoptosis and viability tests

Jurkat cells were seeded in a 24 well plate at 2 × 10E6 cells/ml in 0.5 ml of media. PSG1-Fc and GAL-9 were preincubated at 37 °C for 1 h and then added to the cells. After 24 h treatment, cells were collected, washed, and stained with FITC-Annexin (BioLegend, catalog# 640906) and SYTOX Blue (Thermo Fisher Scientific, catalog# S34857) and analyzed using the BD LSR II (BD Biosciences). Fifty thousand total events were collected for each condition using the FACSDiva software (BD Biosciences, https://www.bdbiosciences.com/en-us/products/software/instrument-software/bd-facsdiva-software), and the FlowJo software (V10.0.8, BD Biosciences, https://www.flowjo.com) was used for postacquisition analysis.

Human $CD4^+$ T cells (bulk and naïve) were purified from PBMCs using EasySep Human $CD4^+$ T Cell Enrichment Kits (Catalog#17952) or Human Naïve CD4+ T Cell Isolation Kits (Catalog#19555) (STEMCELL Technologies) according to the manufacturer's instructions. Cell suspensions were maintained in RPMI-1640 medium containing 10% HI FBS, 1-mM sodium pyruvate, 4.5-g/L glucose, with anti-CD3/CD28 beads, and recombinant hIL-2. Thirty thousand cells per well were seeded in a white flat-bottom plate. PSG1 and GAL-9 were preincubated at 37 °C for 1 h before being added to the T cells. Apoptosis and necrosis were assessed using RealTime-Glo Annexin V Apoptosis and Necrosis Assay (Promega, catalog# JA1011) according to the manufacturer's instructions. Luminescence and fluorescence measurements were recorded using a GloMax plate reader (Promega).

Human cell culture conditions to study Treg conversion

Naïve CD4+ T cells were isolated from PBMCs using a Naïve T Cell Isolation Kit (STEMCELL Technologies, Catalog# 19555). Cells were cultured as stated above in RPMI 1040 with 10% FBS and 100 μg/ml penicillin/streptomycin with anti-CD3/CD28 beads (GenScript, Catalog#L00899) and

recombinant hIL-2 in the presence of the indicated recombinant proteins.

Flow cytometric analysis

Five days after plating, T cells were washed and resuspended in serum and azide-free PBS and were stained with the eFluor 780 Viability dye (eBioscience, Catalog#65–0865–14) for 30 min at 4 °C. Cells were washed and incubated with anti-mouse CD4-FITC (OKT4) and CD25-APC (Thermo Fisher Scientific, Catalog# 88–8999–40) for 30 min at RT. Cells were fixed and permeabilized using the FoxP3 Staining Buffer Set (Thermo Fisher Scientific, Catalog# 88–8999–40), and then stained with anti-mouse FoxP3-PE (Thermo Fisher Scientific, Catalog# 88–8999–40). Human samples were gated for CD4 expression before gating for FoxP3 expression. Samples were run on a benchtop BD FACSymphony A5 Cell Analyzer (BD Biosciences) and analysis was performed using FlowJo FACS analysis software (https://www.flowjo.com).

Statistics

Statistical analyses were performed using a one-tailed two-tailed Student's t test. Posthoc comparisons were performed using Sidak's test. For the comparison of TNF-α levels in human monocytes, we used the Wilcoxon signed-rank test. Data were presented as mean ± SD. All data were analyzed using the Graphpad Prism (https://www.graphpad.com). Differences were considered significant when $p < 0.05$.

Data availability

All data are contained within the manuscript.

Supporting information—This article contains supporting information.

Acknowledgment—We thank Dr S. Jonjic (University of Rijeka) for the anti-PSG antibody MAb#4.

Author contributions—M. M., A. B., E. R.-C., R. T., J. W., S. M. B., and G. D. investigation; M. M., A. B., E. R.-C., J. W., A. L. S., S. R. S., S. M. B., and G. D. writing–review and editing; M. M., A. B., R. T., S. R. S., S. M. B., and G. D. methodology; M. M., A. B., and G. D. writing—original draft; M. M., A. B., and G. D. formal analysis; A. B., A. L. S. and G. D. conceptualization; A. B., S. R. S., S. M. B., and G. D. resources; A. B. and G. D. data curation; A. B. and G. D. visualization; S. M. B., and G. D. funding acquisition; G. D. supervision; G. D. validation; G. D. project administration.

Funding and additional information—This research was supported by the National Institutes of Allergy and Infectious Diseases of the National Institutes of Health (NIH) under award number R21AI156058 (to G. D.) and by grants from the Deutsche Forschungsgemeinschaft (DFG) BL1115/4-1, Heisenberg Program (BL1115/3-1, BL1115/7-1, and BL1115/11-1), and Heike Wolfgang Mühlbauer Stiftung (to S. M. B.). A. B. and R. T. were supported by the Division of Intramural Research of the National Institute of Deafness and Other Communication Disorders (NIDCD DIR DC000096). The opinions expressed here are those of the authors and should not be construed as official or reflecting the views of the Uniformed Services University of the Health Sciences or the Department of Defense.

Conflicts of interest—The authors declare that they have no conflicts of interest with the contents of this article.

Abbreviations—The abbreviations used are: BSA, bovine serum albumin; CRD, carbohydrate recognition domain; FBS, fetal bovine serum; GAL-1, galectin 1; HI, heat inactivated; iTregs, induced Tregs; LPS, lipopolysaccharide; PBMC, peripheral blood mononuclear cell; PSG, pregnancy-specific glycoprotein; SPR, surface plasmon resonance; Tim-3, T-cell immunoglobulin mucin-3; TGF, transforming growth factor; TNF-α, tumor necrosis factor alpha.

References

1. Blois, S. M., Dveksler, G., Vasta, G. R., Freitag, N., Blanchard, V., and Barrientos, G. (2019) Pregnancy galectinology: insights into a complex network of glycan binding proteins. *Front. Immunol.* **10**, 1166
2. Menkhorst, E., Than, N. G., Jeschke, U., Barrientos, G., Szereday, L., Dveksler, G., *et al.* (2021) Medawar's PostEra: galectins emerged as key players during fetal-maternal glycoimmune adaptation. *Front. Immunol.* **12**, 784473
3. Than, N. G., Pick, E., Bellyei, S., Szigeti, A., Burger, O., Berente, Z., *et al.* (2004) Functional analyses of placental protein 13/galectin-13. *Eur. J. Biochem.* **271**, 1065–1078
4. Perillo, N. L., Pace, K. E., Seilhamer, J. J., and Baum, L. G. (1995) Apoptosis of T cells mediated by galectin-1. *Nature* **378**, 736–739
5. Yu, F., Finley, R. L., Jr., Raz, A., and Kim, H. R. (2002) Galectin-3 translocates to the perinuclear membranes and inhibits cytochrome c release from the mitochondria. A role for synexin in galectin-3 translocation. *J. Biol. Chem.* **277**, 15819–15827
6. Yang, R. Y., Hsu, D. K., and Liu, F. T. (1996) Expression of galectin-3 modulates T-cell growth and apoptosis. *Proc. Natl. Acad. Sci. U. S. A.* **93**, 6737–6742
7. Elad-Sfadia, G., Haklai, R., Balan, E., and Kloog, Y. (2004) Galectin-3 augments K-Ras activation and triggers a Ras signal that attenuates ERK but not phosphoinositide 3-kinase activity. *J. Biol. Chem.* **279**, 34922–34930
8. Zhu, C., Anderson, A. C., Schubart, A., Xiong, H., Imitola, J., Khoury, S. J., *et al.* (2005) The Tim-3 ligand galectin-9 negatively regulates T helper type 1 immunity. *Nat. Immunol.* **6**, 1245–1252
9. Wu, C., Thalhamer, T., Franca, R. F., Xiao, S., Wang, C., Hotta, C., *et al.* (2014) Galectin-9-CD44 interaction enhances stability and function of adaptive regulatory T cells. *Immunity* **41**, 270–282
10. Unverdorben, L., Jeschke, U., Santoso, L., Hofmann, S., Kuhn, C., Arck, P., *et al.* (2016) Comparative analyses on expression of galectins1-4, 7-10 and 12 in first trimester placenta, decidua and isolated trophoblast cells in vitro. *Histol. Histopathol.* **31**, 1095–1111
11. Bohn, H., Kraus, W., and Winckler, W. (1983) Purification and characterization of two new soluble placental tissue proteins (PP13 and PP17). *Oncodev. Biol. Med.* **4**, 343–350
12. Maquoi, E., van den Brule, F. A., Castronovo, V., and Foidart, J. M. (1997) Changes in the distribution pattern of galectin-1 and galectin-3 in human placenta correlates with the differentiation pathways of trophoblasts. *Placenta* **18**, 433–439
13. von Wolff, M., Wang, X., Gabius, H. J., and Strowitzki, T. (2005) Galectin fingerprinting in human endometrium and decidua during the menstrual cycle and in early gestation. *Mol. Hum. Reprod.* **11**, 189–194
14. Popovici, R. M., Krause, M. S., Germeyer, A., Strowitzki, T., and von Wolff, M. (2005) Galectin-9: a new endometrial epithelial marker for the mid- and late-secretory and decidual phases in humans. *J. Clin. Endocrinol. Metab.* **90**, 6170–6176
15. Shimizu, Y., Kabir-Salmani, M., Azadbakht, M., Sugihara, K., Sakai, K., and Iwashita, M. (2008) Expression and localization of galectin-9 in the human uterodome. *Endocr. J.* **55**, 879–887

16. Thijssen, V. L., Hulsmans, S., and Griffioen, A. W. (2008) The galectin profile of the endothelium: altered expression and localization in activated and tumor endothelial cells. *Am. J. Pathol.* **172**, 545–553
17. Heusschen, R., Freitag, N., Tirado-Gonzalez, I., Barrientos, G., Moschansky, P., Munoz-Fernandez, R., *et al.* (2013) Profiling Lgals9 splice variant expression at the fetal-maternal interface: implications in normal and pathological human pregnancy. *Biol. Reprod.* **88**, 22
18. Sammar, M., Drobnjak, T., Mandala, M., Gizurarson, S., Huppertz, B., and Meiri, H. (2019) Galectin 13 (PP13) facilitates remodeling and structural stabilization of maternal vessels during pregnancy. *Int. J. Mol. Sci.* **20**, 3192
19. Chen, M., Shi, J. L., Zheng, Z. M., Lin, Z., Li, M. Q., and Shao, J. (2022) Galectins: important regulators in normal and pathologic pregnancies. *Int. J. Mol. Sci.* **23**, 10110
20. Tirado-Gonzalez, I., Freitag, N., Barrientos, G., Shaikly, V., Nagaeva, O., Strand, M., *et al.* (2013) Galectin-1 influences trophoblast immune evasion and emerges as a predictive factor for the outcome of pregnancy. *Mol. Hum. Reprod.* **19**, 43–53
21. Enninga, E. A. L., Harrington, S. M., Creedon, D. J., Ruano, R., Markovic, S. N., Dong, H., *et al.* (2018) Immune checkpoint molecules soluble program death ligand 1 and galectin-9 are increased in pregnancy. *Am. J. Reprod. Immunol.* **79**, e12795
22. Freitag, N., Tirado-Gonzalez, I., Barrientos, G., Powell, K. L., Boehm-Sturm, P., Koch, S. P., *et al.* (2020) Galectin-3 deficiency in pregnancy increases the risk of fetal growth restriction (FGR) *via* placental insufficiency. *Cell Death Dis.* **11**, 560
23. Huppertz, B., Sammar, M., Chefetz, I., Neumaier-Wagner, P., Bartz, C., and Meiri, H. (2008) Longitudinal determination of serum placental protein 13 during development of preeclampsia. *Fetal Diagn. Ther.* **24**, 230–236
24. Wada, J., and Kanwar, Y. S. (1997) Identification and characterization of galectin-9, a novel beta-galactoside-binding mammalian lectin. *J. Biol. Chem.* **272**, 6078–6086
25. Kandel, S., Adhikary, P., Li, G., and Cheng, K. (2021) The TIM3/Gal9 signaling pathway: an emerging target for cancer immunotherapy. *Cancer Lett.* **510**, 67–78
26. Cai, L., Li, Y., Tan, J., Xu, L., and Li, Y. (2023) Targeting LAG-3, TIM-3, and TIGIT for cancer immunotherapy. *J. Hematol. Oncol.* **16**, 101
27. Dixon, K. O., Tabaka, M., Schramm, M. A., Xiao, S., Tang, R., Dionne, D., *et al.* (2021) TIM-3 restrains anti-tumour immunity by regulating inflammasome activation. *Nature* **595**, 101–106
28. Tang, R., Rangachari, M., and Kuchroo, V. K. (2019) Tim-3: a co-receptor with diverse roles in T cell exhaustion and tolerance. *Semin. Immunol.* **42**, 101302
29. Zhao, J., Lei, Z., Liu, Y., Li, B., Zhang, L., Fang, H., *et al.* (2009) Human pregnancy up-regulates Tim-3 in innate immune cells for systemic immunity. *J. Immunol.* **182**, 6618–6624
30. Gleason, M. K., Lenvik, T. R., McCullar, V., Felices, M., O'Brien, M. S., Cooley, S. A., *et al.* (2012) Tim-3 is an inducible human natural killer cell receptor that enhances interferon gamma production in response to galectin-9. *Blood* **119**, 3064–3072
31. Katoh, S., Ishii, N., Nobumoto, A., Takeshita, K., Dai, S. Y., Shinonaga, R., *et al.* (2007) Galectin-9 inhibits CD44-hyaluronan interaction and suppresses a murine model of allergic asthma. *Am. J. Respir. Crit. Care Med.* **176**, 27–35
32. Moore, T., Williams, J. M., Becerra-Rodriguez, M. A., Dunne, M., Kammerer, R., and Dveksler, G. (2022) Pregnancy-specific glycoproteins: evolution, expression, functions and disease associations. *Reproduction* **163**, R11–R23
33. Towler, C. M., Horne, C. H., Jandial, V., Campbell, D. M., and MacGillivray, I. (1976) Plasma levels of pregnancy-specific beta1-glycoprotein in normal pregnancy. *Br. J. Obstet. Gynaecol.* **83**, 775–779
34. Towler, C. M., Horne, C. H., Jandial, V., Campbell, D. M., and MacGillivray, I. (1977) Plasma levels of pregnancy-specific beta 1-glycoprotein in complicated pregnancies. *Br. J. Obstet. Gynaecol.* **84**, 258–263
35. Rattila, S., Dunk, C. E. E., Im, M., Grichenko, O., Zhou, Y., Yanez-Mo, M., *et al.* (2019) Interaction of pregnancy-specific glycoprotein 1 with integrin Alpha5beta1 is a modulator of extravillous trophoblast functions. *Cells* **8**, 1369
36. Kammerer, R., and Zimmermann, W. (2023) Two waves of evolution in the rodent pregnancy-specific glycoprotein (Psg) gene family lead to structurally diverse PSGs. *BMC Genomics* **24**, 468
37. Moore, T., and Dveksler, G. S. (2014) Pregnancy-specific glycoproteins: complex gene families regulating maternal-fetal interactions. *Int. J. Dev. Biol.* **58**, 273–280
38. Zebhauser, R., Kammerer, R., Eisenried, A., McLellan, A., Moore, T., and Zimmermann, W. (2005) Identification of a novel group of evolutionarily conserved members within the rapidly diverging murine Cea family. *Genomics* **86**, 566–580
39. Chuong, E. B., Tong, W., and Hoekstra, H. E. (2010) Maternal-fetal conflict: rapidly evolving proteins in the rodent placenta. *Mol. Biol. Evol.* **27**, 1221–1225
40. Zimmermann, W., and Kammerer, R. (2021) The immune-modulating pregnancy-specific glycoproteins evolve rapidly and their presence correlates with hemochorial placentation in primates. *BMC Genomics* **22**, 128
41. Shanley, D. K., Kiely, P. A., Golla, K., Allen, S., Martin, K., O'Riordan, R. T., *et al.* (2013) Pregnancy-specific glycoproteins bind integrin alphaIIb-beta3 and inhibit the platelet-fibrinogen interaction. *PLoS One* **8**, e57491
42. Blois, S. M., Tirado-Gonzalez, I., Wu, J., Barrientos, G., Johnson, B., Warren, J., *et al.* (2012) Early expression of pregnancy-specific glycoprotein 22 (PSG22) by trophoblast cells modulates angiogenesis in mice. *Biol. Reprod.* **86**, 191
43. Wu, J. A., Johnson, B. L., Chen, Y., Ha, C. T., and Dveksler, G. S. (2008) Murine pregnancy-specific glycoprotein 23 induces the proangiogenic factors transforming-growth factor beta 1 and vascular endothelial growth factor a in cell types involved in vascular remodeling in pregnancy. *Biol. Reprod.* **79**, 1054–1061
44. Rattila, S., Kleefeldt, F., Ballesteros, A., Beltrame, J. S., M, L. R., Ergun, S., *et al.* (2020) Pro-angiogenic effects of pregnancy-specific glycoproteins in endothelial and extravillous trophoblast cells. *Reproduction* **160**, 737–750
45. Warren, J., Im, M., Ballesteros, A., Ha, C., Moore, T., Lambert, F., *et al.* (2018) Activation of latent transforming growth factor-beta1, a conserved function for pregnancy-specific beta 1-glycoproteins. *Mol. Hum. Reprod.* **24**, 602–612
46. McLellan, A. S., Fischer, B., Dveksler, G., Hori, T., Wynne, F., Ball, M., *et al.* (2005) Structure and evolution of the mouse pregnancy-specific glycoprotein (Psg) gene locus. *BMC Genomics* **6**, 4
47. Mendoza, M., Lu, D., Ballesteros, A., Blois, S. M., Abernathy, K., Feng, C., *et al.* (2020) Glycan characterization of pregnancy-specific glycoprotein 1 and its identification as a novel Galectin-1 ligand. *Glycobiology* **30**, 895–909
48. Stowell, S. R., Cho, M., Feasley, C. L., Arthur, C. M., Song, X., Colucci, J. K., *et al.* (2009) Ligand reduces galectin-1 sensitivity to oxidative inactivation by enhancing dimer formation. *J. Biol. Chem.* **284**, 4989–4999
49. Ball, M., McLellan, A., Collins, B., Coadwell, J., Stewart, F., and Moore, T. (2004) An abundant placental transcript containing an IAP-LTR is allelic to mouse pregnancy-specific glycoprotein 23 (Psg23): cloning and genetic analysis. *Gene* **325**, 103–113
50. Nishi, N., Itoh, A., Shoji, H., Miyanaka, H., and Nakamura, T. (2006) Galectin-8 and galectin-9 are novel substrates for thrombin. *Glycobiology* **16**, 15C–20C
51. Yang, R. Y., Rabinovich, G. A., and Liu, F. T. (2008) Galectins: structure, function and therapeutic potential. *Expert Rev. Mol. Med.* **10**, e17
52. Hirabayashi, J., Hashidate, T., Arata, Y., Nishi, N., Nakamura, T., Hirashima, M., *et al.* (2002) Oligosaccharide specificity of galectins: a search by frontal affinity chromatography. *Biochim. Biophys. Acta* **1572**, 232–254
53. Li, Y., Feng, J., Geng, S., Geng, S., Wei, H., Chen, G., *et al.* (2011) The N- and C-terminal carbohydrate recognition domains of galectin-9 contribute differently to its multiple functions in innate immunity and adaptive immunity. *Mol. Immunol.* **48**, 670–677
54. Anderson, A. C., Anderson, D. E., Bregoli, L., Hastings, W. D., Kassam, N., Lei, C., *et al.* (2007) Promotion of tissue inflammation by the immune

receptor Tim-3 expressed on innate immune cells. *Science* **318**, 1141–1143
55. Hao, H., He, M., Li, J., Zhou, Y., Dang, J., Li, F., *et al.* (2015) Upregulation of the Tim-3/Gal-9 pathway and correlation with the development of preeclampsia. *Eur. J. Obstet. Gynecol. Reprod. Biol.* **194**, 85–91
56. Yasinska, I. M., Meyer, N. H., Schlichtner, S., Hussain, R., Siligardi, G., Casely-Hayford, M., *et al.* (2020) Ligand-receptor interactions of galectin-9 and VISTA suppress human T lymphocyte cytotoxic activity. *Front. Immunol.* **11**, 580557
57. Hastings, W. D., Anderson, D. E., Kassam, N., Koguchi, K., Greenfield, E. A., Kent, S. C., *et al.* (2009) TIM-3 is expressed on activated human CD4+ T cells and regulates Th1 and Th17 cytokines. *Eur. J. Immunol.* **39**, 2492–2501
58. Wang, F., He, W., Zhou, H., Yuan, J., Wu, K., Xu, L., *et al.* (2007) The Tim-3 ligand galectin-9 negatively regulates CD8+ alloreactive T cell and prolongs survival of skin graft. *Cell Immunol.* **250**, 68–74
59. Su, E. W., Bi, S., and Kane, L. P. (2011) Galectin-9 regulates T helper cell function independently of Tim-3. *Glycobiology* **21**, 1258–1265
60. Yang, R., Sun, L., Li, C. F., Wang, Y. H., Yao, J., Li, H., *et al.* (2021) Galectin-9 interacts with PD-1 and TIM-3 to regulate T cell death and is a target for cancer immunotherapy. *Nat. Commun.* **12**, 832
61. Lhuillier, C., Barjon, C., Niki, T., Gelin, A., Praz, F., Morales, O., *et al.* (2015) Impact of exogenous galectin-9 on human T cells: contribution of the T cell receptor complex to antigen-independent activation but not to apoptosis induction. *J. Biol. Chem.* **290**, 16797–16811
62. Lv, K., Zhang, Y., Zhang, M., Zhong, M., and Suo, Q. (2013) Galectin-9 promotes TGF-beta1-dependent induction of regulatory T cells *via* the TGF-beta/Smad signaling pathway. *Mol. Med. Rep.* **7**, 205–210
63. Bonney, E. A., and Johnson, M. R. (2019) The role of maternal T cell and macrophage activation in preterm birth: cause or consequence? *Placenta* **79**, 53–61
64. Wolf, Y., Anderson, A. C., and Kuchroo, V. K. (2020) TIM3 comes of age as an inhibitory receptor. *Nat. Rev. Immunol.* **20**, 173–185
65. Troncoso, M. F., Elola, M. T., Blidner, A. G., Sarrias, L., Espelt, M. V., and Rabinovich, G. A. (2023) The universe of galectin-binding partners and their functions in health and disease. *J. Biol. Chem.* **299**, 105400
66. Gonçalves Silva, I., Yasinska, I. M., Sakhnevych, S. S., Fiedler, W., Wellbrock, J., Bardelli, M., *et al.* (2017) The tim-3-galectin-9 secretory pathway is involved in the immune escape of human acute myeloid leukemia cells. *EBioMedicine* **22**, 44–57
67. Prokhorov, A., Gibbs, B. F., Bardelli, M., Rüegg, L., Fasler-Kan, E., Varani, L., *et al.* (2015) The immune receptor Tim-3 mediates activation of PI3 kinase/mTOR and HIF-1 pathways in human myeloid leukaemia cells. *Int. J. Biochem. Cell Biol.* **59**, 11–20
68. Bitra, A., Doukov, T., Wang, J., Picarda, G., Benedict, C. A., Croft, M., *et al.* (2018) Crystal structure of murine 4-1BB and its interaction with 4-1BBL support a role for galectin-9 in 4-1BB signaling. *J. Biol. Chem.* **293**, 1317–1329
69. Enninga, E. A. L., Chatzopoulos, K., Butterfield, J. T., Sutor, S. L., Leontovich, A. A., Nevala, W. K., *et al.* (2018) CD206-positive myeloid cells bind galectin-9 and promote a tumor-supportive microenvironment. *J. Pathol.* **245**, 468–477
70. Sudhakar, J. N., Lu, H. H., Chiang, H. Y., Suen, C. S., Hwang, M. J., Wu, S. Y., *et al.* (2020) Lumenal Galectin-9-Lamp2 interaction regulates lysosome and autophagy to prevent pathogenesis in the intestine and pancreas. *Nat. Commun.* **11**, 4286
71. Schlichtner, S., Meyer, N. H., Yasinska, I. M., Aliu, N., Berger, S. M., Gibbs, B. F., *et al.* (2021) Functional role of galectin-9 in directing human innate immune reactions to Gram-negative bacteria and T cell apoptosis. *Int. Immunopharmacol.* **100**, 108155
72. Daley, D., Mani, V. R., Mohan, N., Akkad, N., Ochi, A., Heindel, D. W., *et al.* (2017) Dectin 1 activation on macrophages by galectin 9 promotes pancreatic carcinoma and peritumoral immune tolerance. *Nat. Med.* **23**, 556–567
73. Matsuura, A., Tsukada, J., Mizobe, T., Higashi, T., Mouri, F., Tanikawa, R., *et al.* (2009) Intracellular galectin-9 activates inflammatory cytokines in monocytes. *Genes Cells* **14**, 511–521
74. Shapourian, H., Ghanadian, M., Eskandari, N., Shokouhi, A., Demirel, G. Y., Bazhin, A. V., *et al.* (2024) TIM-3/Galectin-9 interaction and glutamine metabolism in AML cell lines, HL-60 and THP-1. *BMC Cancer* **24**, 125
75. Tureci, O., Schmitt, H., Fadle, N., Pfreundschuh, M., and Sahin, U. (1997) Molecular definition of a novel human galectin which is immunogenic in patients with Hodgkin's disease. *J. Biol. Chem.* **272**, 6416–6422
76. Blenda, A. V., Kamili, N. A., Wu, S. C., Abel, W. F., Ayona, D., Gerner-Smidt, C., *et al.* (2022) Galectin-9 recognizes and exhibits antimicrobial activity toward microbes expressing blood group-like antigens. *J. Biol. Chem.* **298**, 101704
77. John, S., and Mishra, R. (2016) Galectin-9: from cell biology to complex disease dynamics. *J. Biosci.* **41**, 507–534
78. Lu, L. H., Nakagawa, R., Kashio, Y., Ito, A., Shoji, H., Nishi, N., *et al.* (2007) Characterization of galectin-9-induced death of Jurkat T cells. *J. Biochem.* **141**, 157–172
79. Ji, X. J., Ma, C. J., Wang, J. M., Wu, X. Y., Niki, T., Hirashima, M., *et al.* (2013) HCV-infected hepatocytes drive CD4+ CD25+ Foxp3+ regulatory T-cell development through the Tim-3/Gal-9 pathway. *Eur. J. Immunol.* **43**, 458–467
80. Babbage, S. J., Arkwright, P. D., Vince, G. S., Perrey, C., Pravica, V., Quenby, S., *et al.* (2001) Cytokine promoter gene polymorphisms and idiopathic recurrent pregnancy loss. *J. Reprod. Immunol.* **51**, 21–27
81. Anim-Nyame, N., Gamble, J., Sooranna, S. R., Johnson, M. R., and Steer, P. J. (2003) Microvascular permeability is related to circulating levels of tumour necrosis factor-alpha in pre-eclampsia. *Cardiovasc. Res.* **58**, 162–169
82. Wang, W., Sung, N., Gilman-Sachs, A., and Kwak-Kim, J. (2020) T helper (Th) cell profiles in pregnancy and recurrent pregnancy losses: Th1/Th2/Th9/Th17/Th22/tfh cells. *Front. Immunol.* **11**, 2025
83. Kopcow, H. D., Rosetti, F., Leung, Y., Allan, D. S., Kutok, J. L., and Strominger, J. L. (2008) T cell apoptosis at the maternal-fetal interface in early human pregnancy, involvement of galectin-1. *Proc. Natl. Acad. Sci. U. S. A.* **105**, 18472–18477
84. Zhao, F., Tallarek, A. C., Wang, Y., Xie, Y., Diemert, A., Lu-Culligan, A., *et al.* (2023) A unique maternal and placental galectin signature upon SARS-CoV-2 infection suggests galectin-1 as a key alarmin at the maternal-fetal interface. *Front. Immunol.* **14**, 1196395
85. Menkhorst, E., Koga, K., Van Sinderen, M., and Dimitriadis, E. (2014) Galectin-7 serum levels are altered prior to the onset of pre-eclampsia. *Placenta* **35**, 281–285
86. Su, J., Wang, Y., Si, Y., Gao, J., Song, C., Cui, L., *et al.* (2018) Galectin-13, a different prototype galectin, does not bind β-galacto-sides and forms dimers *via* intermolecular disulfide bridges between Cys-136 and Cys-138. *Sci. Rep.* **8**, 980
87. Than, N. G., Romero, R., Kim, C. J., McGowen, M. R., Papp, Z., and Wildman, D. E. (2012) Galectins: guardians of eutherian pregnancy at the maternal–fetal interface. *Trends Endocrinol. Metab.* **23**, 23–31
88. Than, N. G., Balogh, A., Romero, R., Kárpáti, É., Erez, O., Szilágyi, A., *et al.* (2014) Placental protein 13 (PP13) – a placental immunoregulatory galectin protecting pregnancy. *Front. Immunol.* **5**, 348
89. Deng, Y., Efremov, A. K., and Yan, J. (2022) Modulating binding affinity, specificity, and configurations by multivalent interactions. *Biophys. J.* **121**, 1868–1880
90. Meggyes, M., Miko, E., Polgar, B., Bogar, B., Farkas, B., Illes, Z., *et al.* (2014) Peripheral blood TIM-3 positive NK and CD8+ T cells throughout pregnancy: TIM-3/galectin-9 interaction and its possible role during pregnancy. *PLoS One* **9**, e92371
91. Mittelberger, J., Seefried, M., Franitza, M., Garrido, F., Ditsch, N., Jeschke, U., *et al.* (2022) The role of the immune checkpoint molecules PD-1/PD-L1 and TIM-3/gal-9 in the pathogenesis of preeclampsia-A narrative review. *Medicina (Kaunas)* **58**, 157
92. McLellan, A. S., Zimmermann, W., and Moore, T. (2005) Conservation of pregnancy-specific glycoprotein (PSG) N domains following independent expansions of the gene families in rodents and primates. *BMC Evol. Biol.* **5**, 39
93. Sulkowski, G. N., Warren, J., Ha, C. T., and Dveksler, G. S. (2011) Characterization of receptors for murine pregnancy specific glycoproteins 17 and 23. *Placenta* **32**, 603–610

94. Yung, H. W., Zhao, X., Glover, L., Burrin, C., Pang, P. C., Jones, C. J. P., *et al.* (2023) Perturbation of placental protein glycosylation by endoplasmic reticulum stress promotes maladaptation of maternal hepatic glucose metabolism. *iScience* **26**, 105911
95. Mi, Y., Lin, A., Fiete, D., Steirer, L., and Baenziger, J. U. (2014) Modulation of mannose and asialoglycoprotein receptor expression determines glycoprotein hormone half-life at critical points in the reproductive cycle. *J. Biol. Chem.* **289**, 12157–12167
96. Ballesteros, A., Mentink-Kane, M. M., Warren, J., Kaplan, G. G., and Dveksler, G. S. (2015) Induction and activation of latent transforming growth factor-beta1 are carried out by two distinct domains of pregnancy-specific glycoprotein 1 (PSG1). *J. Biol. Chem.* **290**, 4422–4431